

# 000 001 002 003 004 005 006 007 008 009 010 011 012 013 014 015 016 017 018 019 020 021 022 023 024 025 026 027 028 029 030 031 032 033 034 035 036 037 038 039 040 041 042 043 044 045 046 047 048 049 050 051 052 053 LEARNING REPRESENTATIONS THROUGH CONTRASTIVE NEURAL MODEL CHECKING

Anonymous authors

Paper under double-blind review

## ABSTRACT

Model checking is a key technique for verifying safety-critical systems against formal specifications, where recent applications of deep learning have shown promise. However, while ubiquitous for vision and language domains, representation learning remains underexplored in formal verification. We introduce Contrastive Neural Model Checking (CNML), a novel method that leverages the model checking task as a guiding signal for learning aligned representations. CNML jointly embeds logical specifications and systems into a shared latent space through a self-supervised contrastive objective. On industry-inspired retrieval tasks, CNML considerably outperforms both algorithmic and neural baselines in cross-modal and intra-modal settings. We further show that the learned representations effectively transfer to downstream tasks and generalize to more complex formulas. These findings demonstrate that model checking can serve as an objective for learning representations for formal languages.

## 1 INTRODUCTION

Design errors or flaws, particularly in hardware or safety-critical systems, can result in large financial and reputational damage (Baier & Katoen, 2008). To combat this, formal verification methods are deeply integrated into most modern Electronic Design Automation (EDA) tools and are used by many major software and hardware design companies. One of the main verification paradigms for proving system properties is model checking. It has been used to verify drivers, communication protocols, real-time systems, and many other applications (Clarke et al., 2018), and its impact has been recognized in academia and industry (Clarke et al., 2009).

However, despite the research and advancements in the field (Clarke & Wang, 2014), limitations such as the state space explosion problem (Clarke et al., 2011) complicate usage of model checking for many real-world scenarios. Concurrently, deep learning has achieved remarkable results in related fields of Boolean Satisfiability (SAT) (Selsam & Bjørner, 2019; Selsam et al., 2019) and theorem proving (Han et al., 2021; Bansal et al., 2019; Paliwal et al., 2020). This has motivated early applications of deep learning to model checking (Giacobbe et al., 2024; Zhu et al., 2019; Xu & Lieberherr, 2022) as well as to other verification tasks (Wu et al., 2024; Luo et al., 2022).

Most of the existing work on deep learning for verification has focused on learning formal tasks, with far less focus being spent on the need for aligned representations. Verification procedures such as model-checking typically involve two distinct formal languages for describing the system and the specification (Baier & Katoen, 2008). While feature engineering methods have shown success when working with a single formal language (Kretínský et al., 2025; Lu et al., 2025), aligning representations over two modalities brings additional challenges to an already difficult domain.

In this paper, we present a novel method for learning aligned representations of formal semantics by using the model checking task as a contrastive learning objective for a bi-encoder model. We present a self-supervised learning approach, which combined with a scalable technique for generating large datasets, enables the *Contrastive Neural Model Checking (CNML)* model to learn aligned representation of two semantics jointly used for verification, aligned in a shared latent space. We demonstrate our method on learning two important semantics used in verification: specifications expressed as formulas in Linear Temporal Logic (LTL) (Pnueli, 1977) and systems represented as sequential circuits in the AIGER format (Brummayer et al., 2007).

054 The architecture and the training objective efficiently use the available dataset, avoiding expensive  
 055 computations needed for a fully supervised approach. The proposed architecture is agnostic to the  
 056 syntax of specifications and systems, which allows for easy transfer to different logics or circuit  
 057 encodings, and removes the need for specialized transformer architectures.

058 We evaluate on example tasks motivated by industry practices, showing high *Recall@1%* and  
 059 *Recall@10%* for both cross-modal and intra-modal tasks, outperforming both algorithmic and neural  
 060 baselines on all metrics. Furthermore, the utility of the learned representations is demonstrated for  
 061 downstream finetuning for related tasks, with CNML successfully learning transferable representa-  
 062 tions. We show that our approach leads to a model that can generalize from simple formulas. We  
 063 further show that the learned embeddings carry information beyond the samples seen in training data,  
 064 and that the model can learn complex semantic concepts without explicit supervision.

065 In this work, we make the following contributions:

- 067 1. We introduce a joint-embedding model architecture based on the model checking task for  
 068 AIGER circuits and LTL specifications, which learns aligned embeddings through a self-  
 069 supervised contrastive approach. We present a simple and efficient method to generate, and  
 070 also augment, model checking datasets.
- 071 2. We demonstrate the ability of the model to learn semantics of both circuits and specification,  
 072 and to learn both cross-modal and intra-modal relationships. We show that our model can  
 073 be used for tasks such as retrieval via similarity search. Furthermore, we show that the  
 074 representations can transfer to downstream tasks.
- 075 3. We show that representations learned on simple specifications generalize to complex formu-  
 076 las and transfer effectively to downstream tasks. This shows that by appropriately structuring  
 077 our learning objective, we can successfully learn aligned representations and the underlying  
 078 semantics.

## 079 2 RELATED WORK

080 Deep Learning has proven itself useful in working with formal logics (Li et al., 2024), with success  
 081 in both automated (Bansal et al., 2019; Paliwal et al., 2020) and interactive theorem proving (Mikula  
 082 et al., 2024; Han et al., 2021), Boolean Satisfiability (SAT) (Selsam & Bjørner, 2019; Selsam et al.,  
 083 2019; Ghanem et al., 2024) and Satisfiability Modulo Theories (SMT) (Balunovic et al., 2018).  
 084 Mikula et al. (2024) in particular effectively use contrastive learning for premise selection in theorem  
 085 proving. Our work differs from this general direction by focusing on temporal logics, which are  
 086 particularly important in verification, and by working on developing aligned representations of  
 087 different semantics - something not explored in the wider field of machine learning for logics.

088 In particular, machine learning has been applied in the domain of Linear-Time Temporal Logic (LTL).  
 089 Most of the existing work has focused on traces (Camacho & McIlraith, 2019; Neider & Gavran,  
 090 2018; Walke et al., 2021; Luo et al., 2022). A transformer-based approach in Hahn et al. (2021) shows  
 091 both the ability of neural generation of propositional assignments and, importantly, the ability of  
 092 transformers to generalize to LTL. Recent work by Kretínský et al. (2025) uses hand-crafted features  
 093 of LTL derived game-arenas to guide an algorithm for synthesis. In contrast to these works, we  
 094 focus on learning representations of LTL formulas, rather than on particular tasks related to traces or  
 095 assignments.

096 Due to the wide usage of AIGER in industry, there has been a large variety of work on developing  
 097 methods for learning the representation of circuits, ranging from GNNs to LLMs (Shi et al., 2024;  
 098 Zheng et al., 2025; Zhu et al., 2022). Recent works by Wu et al. (2025) and Fang et al. (2025) are  
 099 based on learning representations of circuits in alignment with properties of hardware description  
 100 language and hardware circuit code to enable specific tasks in the hardware domain. However, there  
 101 has been limited work in learning representations aligned to formal specifications, with the closest  
 102 being by Lu et al. (2025) which uses graph kernel methods to extract features from circuits and select  
 103 the optimal verification algorithm for the instance.

104 Machine learning research combining circuits and specifications has primarily concentrated on  
 105 neural circuit synthesis and neural model checking. Schmitt et al. (2021) propose a neural approach  
 106 for reactive synthesis (Church, 1963) using hierarchical transformers, while Cosler et al. (2023)

108 demonstrate that transformers can perform circuit repair against a formal specification. Most recently,  
 109 Giacobbe et al. (2024) obtain sound neural model checking by learning ranking functions, but their  
 110 method is targeted at solving individual problem instances. Other approaches recast model checking  
 111 in different paradigms: Xu & Lieberherr (2022) frame it as a run-time problem solved with Monte  
 112 Carlo Tree Search, while Madusanka et al. (2023) treat it as a natural-language-style task. Prior  
 113 work on circuits and specifications has concentrated on learning direct tasks. Our work is primarily  
 114 concerned with using neural model checking as a proxy to learn aligned representations of both  
 115 circuits and specifications.

116

### 117 3 BACKGROUND

118

119 **Linear-Time Temporal Logic (LTL).** Linear-Time Temporal logic (LTL) (Pnueli, 1977) is widely  
 120 adopted in both academic and industrial settings (Baier & Katoen, 2008). It serves as the foundation  
 121 for hardware specification languages like Property Specification Language (PSL) (IEEE-Commission,  
 122 2005) and System-Verilog Assertions (SVA) (IEEE-Commission, 2024) used in industry.

123

124 LTL combines propositional boolean logic operators such as  $\neg, \wedge, \vee, \rightarrow$  with temporal operators such  
 125 as  $\bigcirc$  - *next*,  $\mathcal{U}$  - *until*,  $\Box$  - *always*. Temporal operators enable reasoning about sequences of events.  
 126 As an example, the following simple formula describes that as long as  $i_0$  is true, whenever  $i_1$  does  
 127 not hold, in the next step  $o_1$  should be true.

128

$$\varphi = (\Box i_0) \rightarrow (\Box (\neg i_1 \rightarrow \bigcirc o_1))$$

129

130 As LTL does not have a standard normal form, we work with the *assume-guarantee* format as  
 131 our de-facto normal form. This format syntactically separates assumptions from guarantees, both  
 132 composed of conjunctions of LTL sub-formulas. Guarantees describe behaviors that we want to  
 133 verify in our system and assumptions describe the situations in which guarantee properties have to  
 134 hold. The format is generally given in the form of

135

$$\text{spec} := (\text{assumption}_1 \wedge \dots \wedge \text{assumption}_n) \rightarrow (\text{guarantee}_1 \wedge \dots \wedge \text{guarantee}_m)$$

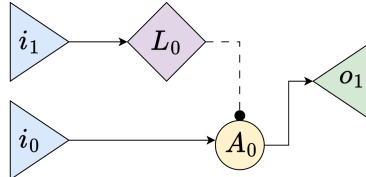
136

137 We provide a complete definition of LTL syntax and semantics in Appendix A.

138

139 **And-Inverter Graphs.** In this paper, we represent sequential circuits as And-Inverter Graphs.  
 140 And-Inverter Graphs, and particularly the ASCII-encoded AIGER (Brummayer et al., 2007), allow  
 141 for a succinct representation of hardware circuits in text form and are widely used in both academia  
 142 and industry. Circuits are built by connecting input variables to output variables through connections  
 143 of logical gates (AND-Gate and NOT-Gate) and memory cells (latches). For a simple example of an  
 144 AND-Inverter Graph and its AIGER representation, see Figure 1. We fully define the AIGER format  
 145 in Appendix B.

146



aag	4	2	1	1	1	header
2						input 0 i_0
4						input 1 i_1
6	4					latch 0 L_0
8						output 0 o_0
8	2	7				and-gate A_0

151

152 Figure 1: Visualization of a simple circuit represented as an And-Inverter Graph and the corresponding  
 153 AIGER text representation. The circuit models the behavior described by the formula  $\varphi$ .

154

155 **Model Checking.** Formally, model checking is an automated way of determining whether a model  
 156 of a system  $S$  satisfies a given formal specification  $\varphi$  of some desired behavior (Clarke et al., 2018).  
 157 The desired behavior is formalized into a specification through some logic such as LTL, CTL, PSL,  
 158 or others. Systems are commonly modeled using circuits or transition systems. A system satisfies  
 159 some property if and only if the specification holds for the output of the circuit for all possible input  
 160 traces. We denote it as  $S \models \varphi$  (system  $S$  satisfies the property  $\varphi$ ).

161

162 Model checking algorithms, in general, have three possible outcomes (Baier & Katoen, 2008). The  
 163 first possible outcome is a result that our specification holds on our model, meaning that the model

162 *satisfies* the specification. The second possible outcome is that the model *violates* the specification,  
 163 in which case the algorithm generates a witness for the behavior of the circuit which violates the  
 164 specification. The third outcome is that the model checking algorithms run out of time and/or memory,  
 165 which happens when the state space of a problem is too large to be handled algorithmically.  
 166

167 **Contrastive Learning.** The main idea of contrastive learning is that models should also learn  
 168 from negative samples, not just the positive ones. Contrastive learning enables the development  
 169 of more robust (Xue et al., 2022) and discriminative representations (Le-Khac et al., 2020). The  
 170 technique’s great success in Computer Vision (Chen et al., 2020; Radford et al., 2021; Khosla et al.,  
 171 2020) motivated its spread into Natural Language Processing, where it has achieved many strong  
 172 results (Wu et al., 2020; Ho & Vasconcelos, 2020; Chen et al., 2020). It has demonstrated capabilities  
 173 in zero-shot learning (Rethmeier & Augenstein, 2023), resilience to noisy datasets (Jia et al., 2021),  
 174 efficacy in transfer learning (Radford et al., 2021), good performance on semantic textual similarity  
 175 tasks (Gao et al., 2021), and generalization to unseen inputs (Pappas & Henderson, 2019) - as well as  
 176 initial use in the logic domain (Mikula et al., 2024; Han et al., 2021).  
 177

## 178 4 DATASET

180 A key driver of the success of modern deep learning, and transformer-based models in particular,  
 181 is the sheer scale of training data (Kaplan et al., 2020). As large datasets of circuit designs are the  
 182 intellectual property of hardware design firms, they are typically kept confidential. Unlike in Natural  
 183 Language Processing, or Computer Vision where data could be scrapped from the internet, there are  
 184 no large circuit-specification datasets available.  
 185

186 As a consequence, we have to synthetically generate a large, high-quality dataset of satisfying pairs.  
 187 However, synthetic data generation is challenging due to the high complexity of the verification  
 188 problem, structure of formal language syntax and semantics, and the need for variety in circuit and  
 189 specification samples.

190 Due to the complexity of the underlying semantics, using purely probabilistic approaches for formula  
 191 generation leads to the generation of syntactically valid formulas that, however, often do not specify  
 192 interesting behaviors. To address this, we follow the LTL formula generation technique from Schmitt  
 193 et al. (2021) to generate a diverse set of LTL formulas. Unlike the works of Schmitt et al. (2021) or  
 194 Cosler et al. (2023), which use the assumptions and guarantees as separate inputs to their hierarchical  
 195 transformers, we generate specifications by merging all assumptions and guarantees into a single LTL  
 196 formula.

197 Generation of corresponding circuits is another significant obstacle, as stochastic methods are unlikely  
 198 to generate satisfying circuits without a very high number of attempts. Therefore, we have to generate  
 199 circuits that inherently satisfy the specification formulas. We use reactive synthesis (Church, 1963) to  
 200 automatically generate satisfying circuits based on each specification. We utilize existing approaches  
 201 and the Strix LTL synthesis tool (Meyer et al., 2018) to create a diverse dataset of satisfying circuits.  
 202

203 To prevent overfitting on syntactic patterns, we perform several augmentations to the data format.  
 204 We shuffle the order of assumption LTL formulas for each specification formula, and we enforce  
 205 a uniform number of input and output wires for all circuits, even if they are not explicitly used.  
 206 Enforcing a fixed number of input and output wires for every circuit eliminates a “wire-counting”  
 207 trick that the model could exploit. By standardizing every circuit to the same number of wires, we  
 208 remove that correlation.

209 We call the resulting dataset with 295,665 samples `cnml-base`.  
 210

## 211 5 LEARNING REPRESENTATIONS

212 The complexity of verification problems (Stockmeyer, 1974; Sistla & Clarke, 1985) presents a  
 213 significant barrier not only to synthetic data generation, but also to learning. As the underlying  
 214 symbolic tasks are highly complex, machine learning models tend to prioritize superficial syntactic  
 215 patterns rather than dealing with the fundamental goal of building semantic understanding.

216 Furthermore, many verification tasks such as model checking, are inherently bimodal - one formal  
 217 language talks about the specification (what we want the system to do) while the second one talks  
 218 about the system model (what the system actually does). While both languages come with their own  
 219 syntax and semantics, they fundamentally describe the same object. This further complicates training  
 220 as the learned representations have to encode not just the properties of their own modality, but also  
 221 the relation to the other one.

222

### 223 5.1 MODEL ARCHITECTURE

224

225 While supervised learning could be used to learn the semantics of verification based on labels derived  
 226 from model checking circuit-specification pairs, this is computationally inefficient as it requires all  
 227 samples to have explicit labels. Furthermore, supervised learning is limited to just one learning  
 228 signal i.e. the label for a single circuit-specification pair. Circuits are not characterized just by the  
 229 specification that they satisfy - but also by the specifications that they do not. This observation  
 230 naturally leads us to contrastive learning, where the learning objective is not defined just by how an  
 231 input relates to its positive samples, in our case circuits and the specifications that they satisfy, but  
 232 also by its relationship with the negative samples - the specifications that they violate. Following  
 233 this idea and inspired by the work of Radford et al. (2021), we adopt a self-supervised contrastive  
 234 approach for learning aligned representations of circuits and formal specifications.

235

236 While Radford et al. (2021) use contrastive learning to align image and text representations, our  
 237 approach adapts this framework to align representations of circuits and specifications. Our model  
 238 is trained to project circuit embeddings closer to the embeddings of specifications they satisfy,  
 239 and farther away from those they do not satisfy. Practically, we view the different semantics and  
 240 syntaxes of circuits and specifications as different modalities, and learn a joint embedding space for  
 241 circuit-specification pairs.

242

243 Our model uses two distinct text encoders,  $E_\varphi$  and  $E_c$ . Despite the encoders learning over a joint  
 244 space,  $E_c$  and  $E_\varphi$  do not share any parameters. While models in related work (Schmitt et al., 2021;  
 245 Cosler et al., 2023; Radford et al., 2021) are trained from scratch, we initialize both encoders as  
 246 CodeBERT models (Feng et al., 2020). As shown by Schmitt et al. (2023) for the closely related task  
 247 of reactive synthesis, pre-trained Transformer models can have a simpler architecture, and achieve  
 248 similar results.

249

250 A single input sample, consisting of a specification and a circuit, is fed into the encoders separately:  
 251  $E_c$  only sees the AIGER circuit  $c$ , and  $E_\varphi$  sees only the LTL specification  $\varphi$ . The forward pass  
 252 through  $E_c$  and  $E_\varphi$  produces the respective input's sequence embeddings. We take the output of the  
 253 pooling of their encodings as the intermediate representation of the whole sequence. Both summary  
 254 vectors are then multiplied by a learned projection matrix (one for  $E_c$  and another for  $E_\varphi$ ), which is  
 255 used to upscale the embedding dimension to 1024.

256

257 The use of two independent encoders forces each one to focus on its own modality. This separation  
 258 prevents overfitting to syntactic patterns that may arise from specific circuit-specification pairings.  
 259 Additionally, the self-supervised approach enables the implicit construction of negative samples  
 260 without requiring explicit model-checking of all possible circuit-specification pairs, which would  
 261 otherwise be computationally infeasible. This allows for generation of a larger corpora, which is  
 262 easier to augment and does not require manual generation of negative samples.

263

### 264 5.2 TRAINING

265

266 At the start of each epoch, we construct the mini-batches using a greedy algorithm. The mini-batches  
 267 are optimized to ensure that they do not contain any duplicate circuits or any duplicate specifications.  
 268 Furthermore, the algorithm cross-checks off-diagonal samples with the rest of the dataset to minimize  
 269 the rate of false negatives which we find to be roughly 4%.

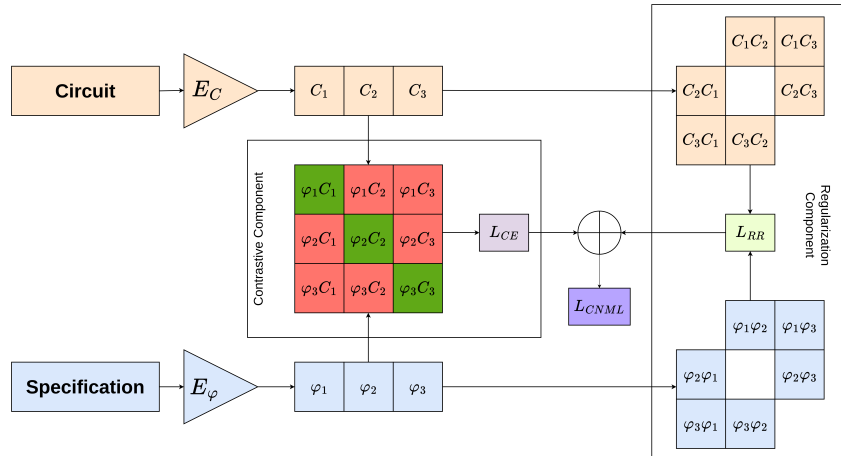
270 Based on  $N$  circuit-specification pairs  $(c_1, \varphi_1), \dots, (c_N, \varphi_N)$  that are directly known to be positive  
 271 ( $c_i$  satisfies  $\varphi_i$ ), we compute the embeddings of circuits and specifications as described previously,  
 272 creating embeddings  $u_{c_1}, \dots, u_{c_N}$  and  $v_{\varphi_1}, \dots, v_{\varphi_N}$ . We then create all pairwise combinations of  
 273 circuit embeddings and specification embeddings  $(u_{c_i}, v_{\varphi_j}), 0 < i, j \leq N$  through a  $N \times N$  matrix.  
 274 Following that, we calculate the cosine similarity for all pairings by computing a dot product between  
 275 all the L2 normalized circuit embeddings and the specification embeddings. On the diagonal of the

270 resulting matrix lie the  $N$  embeddings of circuit-specification pairs  $(c_1, \varphi_1), \dots, (c_N, \varphi_N)$  that are  
 271 directly known to be positive. The remaining  $N^2 - N$  pairs  $(c_i, \varphi_j)$ , where  $i \neq j$  and  $0 < i, j \leq N$ ,  
 272 are implicitly coded negative.

273 The full training objective consists of two components - where  $\mathcal{L}_{\text{CE}}$  is the contrastive component,  
 274 and  $\mathcal{L}_{\text{RR}}$  is the regularization component, with  $\lambda$  being the weighting factor.

$$\mathcal{L}_{\text{CNML}} = \mathcal{L}_{\text{CE}} + \lambda \mathcal{L}_{\text{RR}},$$

275  
 276 The contrastive loss is calculated using a symmetric cross-entropy loss function computed over rows  
 277 and columns of the matrix of similarity scores, following the method from van den Oord et al. (2018).  
 278 We further augment the contrastive loss with a weighted representation similarity regularization loss,  
 279 as introduced in Shi et al. (2023). We find that it provides stability during the training, prevents  
 280 overfitting, and importantly, allows the use of a higher learning rate, without risking catastrophic  
 281 forgetting common in BERT models (Sun et al., 2019; McCloskey & Cohen, 1989). The forward  
 282 pass and loss computation are visualized in Figure 2. We report the hyperparameters and the detailed  
 283 training setup in Appendix C.  
 284



301 Figure 2: Visualization of the forward pass and the computation of the two loss components.  
 302

## 304 6 MODEL EVALUATIONS

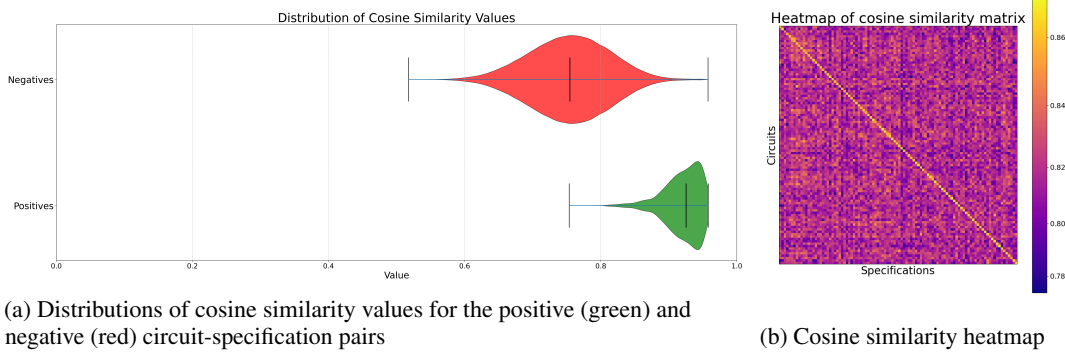
306 We train two models: CNML-base trained on the `cnml-base` dataset for demonstrating the performance  
 307 of our method on various tasks, and CNML-simple trained on the `cnml-split` dataset of  
 308 simple formulas, designed to showcase the model’s ability to generalize (described in detail in Sec-  
 309 tion 6.4). We evaluate the learned embeddings by inspecting the latent space and distribution of cosine  
 310 similarity scores between various circuit-specification pairs, and by assessing performance on two  
 311 retrieval tasks based on real-world problems from Computer-Aided Design, as well as downstream  
 312 fine-tuning for the model checking task.

### 314 6.1 EMBEDDING SPACE ANALYSIS

316 We inspect the learned embedding space by observing the distributions of the cosine similarity that  
 317 our model produces on the test split of `cnml-base`. For a dataset-level insight, Figure 3a plots  
 318 the distributions of cosine similarity values that the model attributes to positive (circuit satisfies the  
 319 specification) and negative (circuit violates the specification) pairs. Both distributions are normalized  
 320 to the probability density function, with the red distribution showing negative, and the green positive  
 321 circuit-specification pairs. For a batch level insight, Figure 3b shows a normalized heatmap of the  
 322 similarity matrix for a singular batch from the test dataset.

323 Both visualizations in Figure 3 show that the model is able to separate satisfying from violating  
 324 pairs of circuits and specification. Figure 3a shows that the model effectively separates the two

324 distributions, with a small remaining overlap. On the heatmap plot, we see that the model produces  
 325 the highest cosine similarity values on the diagonal - the satisfying pairs of circuits and specifications.  
 326  
 327



328 (a) Distributions of cosine similarity values for the positive (green) and  
 329 negative (red) circuit-specification pairs

330 (b) Cosine similarity heatmap

331 Figure 3: Visualization of the Cosine Similarity Distribution produced by the CNML-base model

## 340 6.2 RETRIEVAL

341 We evaluate our model on two retrieval tasks. The first task is *cross-modal* retrieval: given an LTL  
 342 specification, we seek to retrieve a matching design from a collection of candidate circuits. By  
 343 retrieving an existing design, it is possible to avoid the computational expense of automatic synthesis  
 344 or the effort of manual design. Archiving and reusing existing circuits is a common occurrence in  
 345 industry and is supported by many commercial tools (Fang et al., 2025). The second evaluation task  
 346 is an *intra-modal* retrieval task, in which we look for potential optimization replacements for a given  
 347 circuit. Even when an automated tool or an engineer generates a circuit that satisfies the formal  
 348 specification, the result may lack desirable properties such as minimal gate count, wire placement, or  
 349 manufacturability.

350 We generate two test retrieval datasets through mining the test split of `cnml-base`. The first dataset  
 351 consists of 127 test batches, each of size  $N = 100$ , where exactly one circuit is a matching candidate  
 352 while all others do not satisfy the main specification. In the same way, we construct the second  
 353 dataset with 100 test batches of size  $N = 1000$ .

354 We compare the CNML models against several baseline methods. Bag-of-Keywords and Weisfeiler-  
 355 Lehman Graph Kernels (Shervashidze et al., 2011) were recently used for feature extraction of  
 356 circuits in Lu et al. (2025). For a text-edit based similarity metric, we use the Inverted Levenshtein  
 357 distance. For machine-learning baselines we compare against the CodeBert model without any CNML  
 358 pre-training, and against a bi-encoder model following the Sentence-BERT architecture (Reimers &  
 359 Gurevych, 2019), to which we refer as Siamese-CNML.

360 We measure Mean Reciprocal Rank (MRR), Mean Rank (MR) and the *Recall@1%* ( $R@1\%$ ) and  
 361 *Recall@10%* ( $R@10\%$ ) values which measure the recall metric for the top 1% and 10% of the batch,  
 362 respectively. We report the results for cross-modal retrieval in Table 1, and for intra-modal in Table 2.

363 Table 1: Cross-modal Results for Different Methods and Dataset Sizes.

364 Method	365 $127 \times N=100$				366 $100 \times N=1000$			
	367 MRR	368 MR	369 R@1%	370 R@10%	371 MRR	372 MR	373 R@1%	374 R@10%
375 CodeBERT	0.060	46.1	0.8%	4.7%	0.014	471.65	2.0%	9.0%
376 Siamese-CNML	0.043	49.7	0.0%	9.4%	0.005	467.53	1.0%	7.0%
377 CNML-simple	0.118	34.5	4.7%	24.4%	0.099	286.12	15.0%	39.0%
<b>378 CNML-base</b>	<b>0.286</b>	<b>16.6</b>	<b>16.5%</b>	<b>61.4%</b>	<b>0.195</b>	<b>188.03</b>	<b>38.0%</b>	<b>62.0%</b>

378 Table 2: Intra-modal Results for Different Methods and Dataset Sizes.  
379

380 381 382 Method	383 127 × N=100				384 100 × N=1000			
	MRR	385 MR	386 R@1%	387 R@10%	MRR	388 MR	389 R@1%	390 R@10%
Inverted Levenshtein	0.068	49.2	3.1%	11.0%	0.038	472.4	5.0%	12.0%
Bag-of-keywords	0.055	44.2	0.7%	12.6%	0.014	456.1	0.0%	11.0%
Weisfeiler-Lehman	0.066	47.6	2.4%	12.6%	0.023	469.3	7.0%	13.0%
CodeBERT	0.054	50.2	1.6%	9.5%	0.029	468.4	4.0%	12.0%
Siamese-CNML	0.056	48.7	1.6%	8.7%	0.021	456.9	4.0%	16.0%
CNML-simple	0.190	25.9	11.0%	35.4%	0.124	229.6	21.0%	52.0%
<b>CNML-base</b>	<b>0.252</b>	<b>18.9</b>	<b>13.4%</b>	<b>52.7%</b>	<b>0.164</b>	<b>199.8</b>	<b>31.0%</b>	<b>58.0%</b>

391 Results in both tables show that the CNML-base model significantly outperforms all baseline methods  
392 across both scenario sizes. The advantage of CNML-base expands on the larger problem sizes, with  
393 an approximately 75% Mean Rank improvement versus the best algorithmic baseline (Weisfeiler-  
394 Lehman at 417.5). Overall, these results indicate that CNML representations can capture relevant  
395 semantics more effectively than other machine learning or algorithmic approaches, and that they can  
396 be used for tasks directly on the embeddings.

### 398 6.3 DOWNSTREAM FINE-TUNING

400 We further evaluate CNML as a pre-training objective for downstream fine-tuning. We train models  
401 to perform binary classification on circuit-specification pairs to determine whether the circuit  
402 satisfies the specification - the model checking task. The architecture follows the Sentence-Bert  
403 architecture (Reimers & Gurevych, 2019), with the bi-encoders being followed by a linear probe. The  
404 dataset comprises 96940 training examples and 12262 test examples. Models are initialized either  
405 from CodeBERT or from our CNML pre-trained encoders, then fine-tuned on the downstream task.

407 Table 3: Fine-tuning performance on circuit-specification model checking task

409 Model	410 Accuracy	411 Precision	412 Recall	413 F1 Score
CodeBERT	0.830	0.799	0.884	0.839
CNML-simple	0.845	0.814	0.894	0.852
<b>CNML-base</b>	<b>0.887</b>	<b>0.847</b>	<b>0.947</b>	<b>0.894</b>

414 The results in Table 3 demonstrate that CNML pre-training provides substantial benefits for down-  
415 stream performance over the baseline model, where we initialize models with CodeBERT weights  
416 and no CNML pretraining. The performance gain over the baseline CodeBert models, shows that  
417 the contrastive pre-training objective successfully learns transferable representations that capture the  
418 semantic relationship between specifications and circuits.

### 421 6.4 GENERALIZATION

423 We set-up an experiment to test the generalization capabilities of our approach. We evaluate the  
424 generalization capability of CNML models by training on simple formulas and testing on more  
425 complex specifications. To construct a suitable training dataset of circuit-specification pairs, we  
426 employ *formula splitting*. This technique allows us to soundly transform the `cnml-base` dataset  
427 into one with simpler LTL formulas, while preserving the soundness of circuit-specifications pairs.

428 Formula splitting systematically weakens specification guarantees to create new formulas. Consider  
429 an LTL specification  $\varphi$  defined as:

$$430 \varphi := \bigwedge_{assumption \in \varphi_A} assumption \rightarrow \bigwedge_{guarantee \in \varphi_G} guarantee$$

432 where  $\varphi_A$  and  $\varphi_G$  are sets of assumption and guarantee formulas, respectively. For any circuit  $\mathcal{C}$   
 433 satisfying  $\mathcal{C} \models \varphi$  and any guarantee  $\varphi' \in \varphi_G$ , the following holds:  
 434

$$436 \quad \mathcal{C} \models \bigwedge_{assumption \in \varphi_A} assumption \rightarrow \varphi' \\ 437$$

438  
 439 We use this observation, and apply formula splitting to specifications in `cnml-base` while preserving  
 440 the original circuit. By doing this, we generate the `cnml-split` dataset and transform the original  
 441 formulas into ones which contain exactly one guarantee. We train CNML-simple model on this  
 442 dataset, exposing the model only to single-guarantee formulas during training, while evaluating on  
 443 multi-guarantee formulas by using `cnml-base` on the same experiments as with CNML-base.  
 444

445 We evaluate the CNML-simple model on retrieval and fine-tuning tasks. Tables 1 and 2 present  
 446 the performance of CNML-simple on retrieval problems based on specifications more complex  
 447 than the ones seen during training. The model outperforms all baseline methods on both retrieval  
 448 tasks, although performance decreases compared to CNML-base due to the distribution shift and  
 449 the mini-batch noise. Additionally, as shown by fine-tuning results on the model checking task  
 450 (Section 6.3) reported in Table 3, the learned representations transfer to downstream tasks even when  
 451 they involve complex formulas.

452 These results demonstrate that CNML models can generalize from simple training formulas to  
 453 complex multi-guarantee specifications. Since CNML-simple is exposed to only single-guarantee  
 454 formulas during training, its successful performance on multi-guarantee test formulas indicates the  
 455 ability of CNML models to generalize.

## 457 7 CONCLUSION

458 In this paper, we introduced CNML, a neural model checking framework that learns joint embeddings  
 459 of LTL specifications and AIGER circuits. The contrastive self-supervised training approach allows  
 460 for training using only the positive circuit-specification pairs, and can effectively use such samples to  
 461 learn aligned representations of both semantics. We create a large dataset of 295,665 samples and  
 462 present a method for data generation and augmentation at scale, potentially enabling future work  
 463 in machine learning for formal logics and verification - a domain where data is usually scarce and  
 464 computation is prohibitively expensive.

465 Evaluation on industry-inspired retrieval tasks shows that CNML outperforms the baselines, achieving  
 466 high *Recall@1%* and *Recall@10%* for both cross-modal and intra-modal tasks. We further  
 467 demonstrate that the learned representations can be used for fine-tuning on downstream task. We  
 468 show that the method is able to generalize from training on simple formulas, to performing tasks  
 469 on formulas in more complex formats. Our results validate the effectiveness of self-supervised  
 470 contrastive pre-training in learning semantics for used in verification.

471 We believe that the model training paradigm and data generation opens a window for further research  
 472 where representation alignment of formal languages is crucial. The method presented enables learning  
 473 of aligned representation - allowing for future work combining formal methods and deep learning in  
 474 problems such as verification, synthesis and retrieval.

## 478 8 REPRODUCIBILITY STATEMENT

479 We provide detailed information required to reproduce our results. Detailed hyperparameters, training  
 480 set-up and package versions are listed in Appendix C. The dataset generation procedure is described  
 481 in Section 4, while the model architecture and forward pass are detailed in Sections 5.1 and 5.2,  
 482 respectively. We will open-source our implementations, trained model checkpoints, and the dataset  
 483 following the review process.

486 9 LLM’s USE STATEMENT  
487488 During the writing of this paper, Large Language Models were used for the purposes of grammar  
489 checking and correction, as well as to help improve clarity by suggesting text refinements. They were  
490 also used to assist implementation work.  
491492 REFERENCES  
493494 Christel Baier and Joost-Pieter Katoen. *Principles of model checking*. MIT Press, 2008. ISBN  
495 978-0-262-02649-9.  
496497 Mislav Balunovic, Pavol Bielik, and Martin T. Vechev. Learning to solve SMT formulas. In Samy  
498 Bengio, Hanna M. Wallach, Hugo Larochelle, Kristen Grauman, Nicolò Cesa-Bianchi, and Roman  
499 Garnett (eds.), *Advances in Neural Information Processing Systems 31: Annual Conference on  
500 Neural Information Processing Systems 2018, NeurIPS 2018, December 3-8, 2018, Montréal,  
501 Canada*, pp. 10338–10349, 2018. URL <https://proceedings.neurips.cc/paper/2018/hash/68331ff0427b551b68e911eebe35233b-Abstract.html>.  
502503 Kshitij Bansal, Sarah M. Loos, Markus N. Rabe, Christian Szegedy, and Stewart Wilcox. Holist: An  
504 environment for machine learning of higher order logic theorem proving. In Kamalika Chaudhuri  
505 and Ruslan Salakhutdinov (eds.), *Proceedings of the 36th International Conference on Machine  
506 Learning, ICML 2019, 9-15 June 2019, Long Beach, California, USA*, volume 97 of *Proceedings of  
507 Machine Learning Research*, pp. 454–463. PMLR, 2019. URL <http://proceedings.mlr.press/v97/bansal19a.html>.  
508509 R. Brummayer, A. Cimatti, K. Claessen, N. Een, M. Herbstritt, H. Kim, T. Jussila, K. McMillan,  
510 A. Mishchenko, F. Somenzi, et al. The aiger and-inverter graph (aig) format version 20070427,  
511 2007. Available at <http://fmv.jku.at/aiger/>.  
512513 Alberto Camacho and Sheila A. McIlraith. Learning interpretable models expressed in linear temporal  
514 logic. In J. Benton, Nir Lipovetzky, Eva Onaindia, David E. Smith, and Siddharth Srivastava  
515 (eds.), *Proceedings of the Twenty-Ninth International Conference on Automated Planning and  
516 Scheduling, ICAPS 2019, Berkeley, CA, USA, July 11-15, 2019*, pp. 621–630. AAAI Press, 2019.  
517 URL <https://ojs.aaai.org/index.php/ICAPS/article/view/3529>.  
518519 Ting Chen, Simon Kornblith, Mohammad Norouzi, and Geoffrey E. Hinton. A simple framework for  
520 contrastive learning of visual representations. In *Proceedings of the 37th International Conference  
521 on Machine Learning, ICML 2020, 13-18 July 2020, Virtual Event*, volume 119 of *Proceedings  
522 of Machine Learning Research*, pp. 1597–1607. PMLR, 2020. URL <http://proceedings.mlr.press/v119/chen20j.html>.  
523524 Alonzo Church. Application of recursive arithmetic to the problem of circuit synthesis. *Journal of  
525 Symbolic Logic*, 28(4), 1963.  
526527 Edmund M. Clarke and Qinsi Wang. 2<sup>5</sup> years of model checking. In Andrei Voronkov and Irina B.  
528 Virbitskaite (eds.), *Perspectives of System Informatics - 9th International Ershov Informatics  
529 Conference, PSI 2014, St. Petersburg, Russia, June 24-27, 2014. Revised Selected Papers*, vol-  
530 ume 8974 of *Lecture Notes in Computer Science*, pp. 26–40. Springer, 2014. doi: 10.1007/  
531 978-3-662-46823-4\2. URL [https://doi.org/10.1007/978-3-662-46823-4\\_2](https://doi.org/10.1007/978-3-662-46823-4_2).  
532533 Edmund M. Clarke, E. Allen Emerson, and Joseph Sifakis. Model checking: algorithmic verification  
534 and debugging. *Commun. ACM*, 52(11):74–84, 2009. doi: 10.1145/1592761.1592781. URL  
535 <https://doi.org/10.1145/1592761.1592781>.536 Edmund M. Clarke, William Klieber, Milos Novácek, and Paolo Zuliani. Model checking and the  
537 state explosion problem. In Bertrand Meyer and Martin Nordio (eds.), *Tools for Practical Software  
538 Verification, LASER, International Summer School 2011, Elba Island, Italy, Revised Tutorial Lec-  
539 tures*, volume 7682 of *Lecture Notes in Computer Science*, pp. 1–30. Springer, 2011. doi: 10.1007/  
978-3-642-35746-6\1. URL [https://doi.org/10.1007/978-3-642-35746-6\\_1](https://doi.org/10.1007/978-3-642-35746-6_1).  
540

540 Edmund M. Clarke, Thomas A. Henzinger, Helmut Veith, and Roderick Bloem (eds.). *Handbook of*  
 541 *Model Checking*. Springer, 2018. ISBN 978-3-319-10574-1. doi: 10.1007/978-3-319-10575-8.  
 542 URL <https://doi.org/10.1007/978-3-319-10575-8>.

543

544 Matthias Cosler, Frederik Schmitt, Christopher Hahn, and Bernd Finkbeiner. Iterative circuit  
 545 repair against formal specifications. In *The Eleventh International Conference on Learning*  
 546 *Representations, ICLR 2023, Kigali, Rwanda, May 1-5, 2023*. OpenReview.net, 2023. URL  
 547 <https://openreview.net/forum?id=SECsah10Q1>.

548

549 Jacob Devlin, Ming-Wei Chang, Kenton Lee, and Kristina Toutanova. BERT: pre-training of deep  
 550 bidirectional transformers for language understanding, 2019. URL <https://doi.org/10.18653/v1/n19-1423>.

551

552 Alexandre Duret-Lutz, Etienne Renault, Maximilien Colange, Florian Renkin, Alexandre Gbaguidi  
 553 Aisse, Philipp Schlehuber-Caissier, Thomas Medioni, Antoine Martin, Jérôme Dubois, Clément  
 554 Gillard, and Henrich Lauko. From Spot 2.0 to Spot 2.10: What's new? In *Proceedings of*  
 555 *the 34th International Conference on Computer Aided Verification (CAV'22)*, volume 13372  
 556 of *Lecture Notes in Computer Science*, pp. 174–187. Springer, August 2022. doi: 10.1007/978-3-031-13188-2\_9.

557

558 Wenji Fang, Shang Liu, Jing Wang, and Zhiyao Xie. Circuitfusion: Multimodal circuit repre-  
 559 sentation learning for agile chip design. In *The Thirteenth International Conference on Learn-  
 560 ing Representations, ICLR 2025, Singapore, April 24-28, 2025*. OpenReview.net, 2025. URL  
 561 <https://openreview.net/forum?id=rbnf7oe6JQ>.

562

563 Zhangyin Feng, Daya Guo, Duyu Tang, Nan Duan, Xiaocheng Feng, Ming Gong, Linjun Shou, Bing  
 564 Qin, Ting Liu, Daxin Jiang, and Ming Zhou. Codebert: A pre-trained model for programming and  
 565 natural languages. In Trevor Cohn, Yulan He, and Yang Liu (eds.), *Findings of the Association for*  
 566 *Computational Linguistics: EMNLP 2020, Online Event, 16-20 November 2020*, volume EMNLP  
 567 2020 of *Findings of ACL*, pp. 1536–1547. Association for Computational Linguistics, 2020.  
 568 doi: 10.18653/V1/2020.FINDINGS-EMNLP.139. URL <https://doi.org/10.18653/v1/2020.findings-emnlp.139>.

569

570 Tianyu Gao, Xingcheng Yao, and Danqi Chen. Simcse: Simple contrastive learning of sentence  
 571 embeddings. In Marie-Francine Moens, Xuanjing Huang, Lucia Specia, and Scott Wen-tau Yih  
 572 (eds.), *Proceedings of the 2021 Conference on Empirical Methods in Natural Language Processing,*  
 573 *EMNLP 2021, Virtual Event / Punta Cana, Dominican Republic, 7-11 November, 2021*, pp. 6894–  
 574 6910. Association for Computational Linguistics, 2021. doi: 10.18653/V1/2021.EMNLP-MAIN.  
 575 552. URL <https://doi.org/10.18653/v1/2021.emnlp-main.552>.

576

577 Mohamed Ghanem, Frederik Schmitt, Julian Siber, and Bernd Finkbeiner. Learning better repre-  
 578 sentations from less data for propositional satisfiability. In Amir Globersons, Lester Mackey,  
 579 Danielle Belgrave, Angela Fan, Ulrich Paquet, Jakub M. Tomczak, and Cheng Zhang (eds.),  
 580 *Advances in Neural Information Processing Systems 38: Annual Conference on Neural In-  
 581 formation Processing Systems 2024, NeurIPS 2024, Vancouver, BC, Canada, December 10 -  
 582 15, 2024*, 2024. URL [http://papers.nips.cc/paper\\_files/paper/2024/hash/56a225639da77e8f7c0409f6d5ba996b-Abstract-Conference.html](http://papers.nips.cc/paper_files/paper/2024/hash/56a225639da77e8f7c0409f6d5ba996b-Abstract-Conference.html).

583

584 Mirco Giacobbe, Daniel Kroening, Abhinandan Pal, and Michael Tautschnig. Neu-  
 585 ral model checking. In Amir Globersons, Lester Mackey, Danielle Belgrave, Angela  
 586 Fan, Ulrich Paquet, Jakub M. Tomczak, and Cheng Zhang (eds.), *Advances in Neu-  
 587 ral Information Processing Systems 38: Annual Conference on Neural Information Pro-  
 588 cessing Systems 2024, NeurIPS 2024, Vancouver, BC, Canada, December 10 - 15,  
 589 2024*, 2024. URL [http://papers.nips.cc/paper\\_files/paper/2024/hash/9d0947107ea92d6ce369dce7749180dd-Abstract-Conference.html](http://papers.nips.cc/paper_files/paper/2024/hash/9d0947107ea92d6ce369dce7749180dd-Abstract-Conference.html).

590

591 Christopher Hahn, Frederik Schmitt, Jens U. Kreber, Markus Norman Rabe, and Bernd Finkbeiner.  
 592 Teaching temporal logics to neural networks. In *9th International Conference on Learning*  
 593 *Representations, ICLR 2021, Virtual Event, Austria, May 3-7, 2021*. OpenReview.net, 2021. URL  
<https://openreview.net/forum?id=d0cQK-f4byz>.

594 Jesse Michael Han, Tao Xu, Stanislas Polu, Arvind Neelakantan, and Alec Radford. Contrastive  
 595 finetuning of generative language models for informal premise selection. In *6th Conference on*  
 596 *Artificial Intelligence and Theorem Proving*, 2021.

597 Chih-Hui Ho and Nuno Vasconcelos. Contrastive learning with adversarial examples. In  
 598 Hugo Larochelle, Marc'Aurelio Ranzato, Raia Hadsell, Maria-Florina Balcan, and Hsuan-  
 599 Tien Lin (eds.), *Advances in Neural Information Processing Systems 33: Annual Con-*  
 600 *ference on Neural Information Processing Systems 2020, NeurIPS 2020, December 6-12,*  
 601 *2020, virtual*, 2020. URL <https://proceedings.neurips.cc/paper/2020/hash/c68c9c8258ea7d85472dd6fd0015f047-Abstract.html>.

602 IEEE-Commission. IEEE standard for property specification language (PSL). *IEEE Std 1850-2005*,  
 603 2005.

604 IEEE-Commission. Ieee standard for systemverilog—unified hardware design, specification, and  
 605 verification language. *IEEE Std 1800-2023 (Revision of IEEE Std 1800-2017)*, 2024. doi: 10.1109/  
 606 IEEEESTD.2024.10458102.

607 Chao Jia, Yinfei Yang, Ye Xia, Yi-Ting Chen, Zarana Parekh, Hieu Pham, Quoc V. Le, Yun-Hsuan  
 608 Sung, Zhen Li, and Tom Duerig. Scaling up visual and vision-language representation learning  
 609 with noisy text supervision. In Marina Meila and Tong Zhang (eds.), *Proceedings of the 38th*  
 610 *International Conference on Machine Learning, ICML 2021, 18-24 July 2021, Virtual Event*,  
 611 *volume 139 of Proceedings of Machine Learning Research*, pp. 4904–4916. PMLR, 2021. URL  
 612 <http://proceedings.mlr.press/v139/jia21b.html>.

613 Jared Kaplan, Sam McCandlish, Tom Henighan, Tom B. Brown, Benjamin Chess, Rewon Child,  
 614 Scott Gray, Alec Radford, Jeffrey Wu, and Dario Amodei. Scaling laws for neural language models.  
 615 *CoRR*, abs/2001.08361, 2020. URL <https://arxiv.org/abs/2001.08361>.

616 Prannay Khosla, Piotr Teterwak, Chen Wang, Aaron Sarna, Yonglong Tian, Phillip Isola, Aaron  
 617 Maschinot, Ce Liu, and Dilip Krishnan. Supervised contrastive learning. *Advances in neural*  
 618 *information processing systems*, 33:18661–18673, 2020.

619 Jan Kretínský, Tobias Meggendorfer, Maximilian Prokop, and Ashkan Zarkhah. Semml: Enhancing  
 620 automata-theoretic LTL synthesis with machine learning. In Arie Gurfinkel and Marijn Heule  
 621 (eds.), *Tools and Algorithms for the Construction and Analysis of Systems - 31st International*  
 622 *Conference, TACAS 2025, Held as Part of the International Joint Conferences on Theory and*  
 623 *Practice of Software, ETAPS 2025, Hamilton, ON, Canada, May 3-8, 2025, Proceedings, Part I*,  
 624 *volume 15696 of Lecture Notes in Computer Science*, pp. 233–253. Springer, 2025. doi: 10.1007/  
 625 978-3-031-90643-5\12. URL [https://doi.org/10.1007/978-3-031-90643-5\\_12](https://doi.org/10.1007/978-3-031-90643-5_12).

626 Phuc H. Le-Khac, Graham Healy, and Alan F. Smeaton. Contrastive representation learning: A  
 627 framework and review. *IEEE Access*, 8:193907–193934, 2020. doi: 10.1109/ACCESS.2020.  
 628 3031549. URL <https://doi.org/10.1109/ACCESS.2020.3031549>.

629 Zhaoyu Li, Jialiang Sun, Logan Murphy, Qidong Su, Zenan Li, Xian Zhang, Kaiyu Yang, and Xujie  
 630 Si. A survey on deep learning for theorem proving. *CoRR*, abs/2404.09939, 2024. doi: 10.48550/  
 631 ARXIV.2404.09939. URL <https://doi.org/10.48550/arXiv.2404.09939>.

632 Yinhan Liu, Myle Ott, Naman Goyal, Jingfei Du, Mandar Joshi, Danqi Chen, Omer Levy, Mike  
 633 Lewis, Luke Zettlemoyer, and Veselin Stoyanov. Roberta: A robustly optimized BERT pretraining  
 634 approach. *CoRR*, abs/1907.11692, 2019. URL <https://arxiv.org/abs/1907.11692>.

635 Ilya Loshchilov and Frank Hutter. Decoupled weight decay regularization. In *7th International*  
 636 *Conference on Learning Representations, ICLR 2019, New Orleans, LA, USA, May 6-9, 2019*.  
 637 OpenReview.net, 2019. URL <https://openreview.net/forum?id=Bkg6RiCqY7>.

638 Zhengyang Lu, Po-Chun Chien, Nian-Ze Lee, Arie Gurfinkel, and Vijay Ganesh. Btor2-select:  
 639 Machine learning based algorithm selection for hardware model checking. In Ruzica Piskac and  
 640 Zvonimir Rakamaric (eds.), *Computer Aided Verification - 37th International Conference, CAV*  
 641 *2025, Zagreb, Croatia, July 23-25, 2025, Proceedings, Part I*, volume 15931 of *Lecture Notes in*  
 642 *Computer Science*, pp. 296–311. Springer, 2025. doi: 10.1007/978-3-031-98668-0\15. URL  
 643 [https://doi.org/10.1007/978-3-031-98668-0\\_15](https://doi.org/10.1007/978-3-031-98668-0_15).

648 Weilin Luo, Hai Wan, Jianfeng Du, Xiaoda Li, Yuze Fu, Rongzhen Ye, and Delong Zhang. Teaching  
 649 ltlf satisfiability checking to neural networks. In Luc De Raedt (ed.), *Proceedings of the Thirty-*  
 650 *First International Joint Conference on Artificial Intelligence, IJCAI 2022, Vienna, Austria, 23-*  
 651 *29 July 2022*, pp. 3292–3298. ijcai.org, 2022. doi: 10.24963/IJCAI.2022/457. URL <https://doi.org/10.24963/ijcai.2022/457>.

653 Tharindu Madusanka, Riza Theresa Batista-Navarro, and Ian Pratt-Hartmann. Identifying the limits  
 654 of transformers when performing model-checking with natural language. In Andreas Vlachos  
 655 and Isabelle Augenstein (eds.), *Proceedings of the 17th Conference of the European Chapter*  
 656 *of the Association for Computational Linguistics, EACL 2023, Dubrovnik, Croatia, May 2-6,*  
 657 *2023*, pp. 3521–3532. Association for Computational Linguistics, 2023. doi: 10.18653/V1/2023.  
 658 EACL-MAIN.257. URL <https://doi.org/10.18653/v1/2023.eacl-main.257>.

659 Zohar Manna and Amir Pnueli. A hierarchy of temporal properties. In Cynthia Dwork (ed.),  
 660 *Proceedings of the Ninth Annual ACM Symposium on Principles of Distributed Computing, Quebec*  
 661 *City, Quebec, Canada, August 22-24, 1990*, pp. 377–410. ACM, 1990. doi: 10.1145/93385.93442.  
 662 URL <https://doi.org/10.1145/93385.93442>.

664 Michael McCloskey and Neal J Cohen. Catastrophic interference in connectionist networks: The  
 665 sequential learning problem. In *Psychology of learning and motivation*, volume 24, pp. 109–165.  
 666 Elsevier, 1989.

667 Philipp J. Meyer, Salomon Sickert, and Michael Luttenberger. Strix: Explicit reactive synthesis  
 668 strikes back! In *Computer Aided Verification - 30th International Conference, CAV 2018, Held as*  
 669 *Part of the Federated Logic Conference, FloC 2018, Oxford, UK, July 14-17, 2018, Proceedings,*  
 670 *Part I*, volume 10981 of *Lecture Notes in Computer Science*, pp. 578–586. Springer, 2018. doi:  
 671 [10.1007/978-3-319-96145-3\31](https://doi.org/10.1007/978-3-319-96145-3\31).

672 Paulius Micikevicius, Sharan Narang, Jonah Alben, Gregory F. Diamos, Erich Elsen, David García,  
 673 Boris Ginsburg, Michael Houston, Oleksii Kuchaiev, Ganesh Venkatesh, and Hao Wu. Mixed  
 674 precision training. *CoRR*, abs/1710.03740, 2017. URL <http://arxiv.org/abs/1710.03740>.

675 Maciej Mikula, Szymon Tworkowski, Szymon Antoniak, Bartosz Piotrowski, Albert Q. Jiang,  
 676 Jin Peng Zhou, Christian Szegedy, Lukasz Kucinski, Piotr Milos, and Yuhuai Wu. Magnushammer:  
 677 A transformer-based approach to premise selection. In *The Twelfth International Conference on*  
 678 *Learning Representations, ICLR 2024, Vienna, Austria, May 7-11, 2024*. OpenReview.net, 2024.  
 679 URL <https://openreview.net/forum?id=oYjPk8mqAV>.

680 Daniel Neider and Ivan Gavran. Learning linear temporal properties. In Nikolaj S. Bjørner and Arie  
 681 Gurfinkel (eds.), *2018 Formal Methods in Computer Aided Design, FMCAD 2018, Austin, TX, USA,*  
 682 *October 30 - November 2, 2018*, pp. 1–10. IEEE, 2018. doi: 10.23919/FMCAD.2018.8603016.  
 683 URL <https://doi.org/10.23919/FMCAD.2018.8603016>.

684 Aditya Paliwal, Sarah M. Loos, Markus N. Rabe, Kshitij Bansal, and Christian Szegedy. Graph  
 685 representations for higher-order logic and theorem proving. In *The Thirty-Fourth AAAI Conference*  
 686 *on Artificial Intelligence, AAAI 2020, The Thirty-Second Innovative Applications of Artificial*  
 687 *Intelligence Conference, IAAI 2020, The Tenth AAAI Symposium on Educational Advances in*  
 688 *Artificial Intelligence, EAAI 2020, New York, NY, USA, February 7-12, 2020*, pp. 2967–2974.  
 689 AAAI Press, 2020. doi: 10.1609/AAAI.V34I03.5689. URL <https://doi.org/10.1609/aaai.v34i03.5689>.

690 Nikolaos Pappas and James Henderson. GILE: A generalized input-label embedding for text classi-  
 691 fication. *Trans. Assoc. Comput. Linguistics*, 7:139–155, 2019. doi: 10.1162/TACL\_A\_00259.  
 692 URL [https://doi.org/10.1162/tacl\\_a\\_00259](https://doi.org/10.1162/tacl_a_00259).

693 Adam Paszke, Sam Gross, Francisco Massa, Adam Lerer, James Bradbury, Gregory Chanan,  
 694 Trevor Killeen, Zeming Lin, Natalia Gimelshein, Luca Antiga, Alban Desmaison, Andreas  
 695 Köpf, Edward Z. Yang, Zachary DeVito, Martin Raison, Alykhan Tejani, Sasank Chilamkurthy,  
 696 Benoit Steiner, Lu Fang, Junjie Bai, and Soumith Chintala. Pytorch: An imperative style,  
 697 high-performance deep learning library. In Hanna M. Wallach, Hugo Larochelle, Alina  
 698 Beygelzimer, Florence d’Alché-Buc, Emily B. Fox, and Roman Garnett (eds.), *Advances in*

702        *Neural Information Processing Systems 32: Annual Conference on Neural Information Pro-*  
 703        *cessing Systems 2019, NeurIPS 2019, December 8-14, 2019, Vancouver, BC, Canada, pp.*  
 704        *8024–8035. 2019. URL <https://proceedings.neurips.cc/paper/2019/hash/bdbca288fee7f92f2bfa9f7012727740-Abstract.html>.*

705

706        Amir Pnueli. The temporal logic of programs. In *18th Annual Symposium on Foundations of*  
 707        *Computer Science, Providence, Rhode Island, USA, 31 October - 1 November 1977*, pp. 46–57.  
 708        IEEE Computer Society, 1977. doi: 10.1109/SFCS.1977.32. URL <https://doi.org/10.1109/SFCS.1977.32>.

709

710

711        Alec Radford, Jong Wook Kim, Chris Hallacy, Aditya Ramesh, Gabriel Goh, Sandhini Agarwal,  
 712        Girish Sastry, Amanda Askell, Pamela Mishkin, Jack Clark, Gretchen Krueger, and Ilya Sutskever.  
 713        Learning transferable visual models from natural language supervision. In Marina Meila and  
 714        Tong Zhang (eds.), *Proceedings of the 38th International Conference on Machine Learning, ICML 2021, 18-24 July 2021, Virtual Event*, volume 139 of *Proceedings of Machine Learning Research*, pp. 8748–8763. PMLR, 2021. URL <http://proceedings.mlr.press/v139/radford21a.html>.

715

716

717

718        Nils Reimers and Iryna Gurevych. Sentence-bert: Sentence embeddings using siamese bert-networks.  
 719        In Kentaro Inui, Jing Jiang, Vincent Ng, and Xiaojun Wan (eds.), *Proceedings of the 2019*  
 720        *Conference on Empirical Methods in Natural Language Processing and the 9th International*  
 721        *Joint Conference on Natural Language Processing, EMNLP-IJCNLP 2019, Hong Kong, China,*  
 722        *November 3-7, 2019*, pp. 3980–3990. Association for Computational Linguistics, 2019. doi:  
 723        10.18653/V1/D19-1410. URL <https://doi.org/10.18653/v1/D19-1410>.

724

725        Nils Rethmeier and Isabelle Augenstein. A primer on contrastive pretraining in language processing:  
 726        Methods, lessons learned, and perspectives. *ACM Comput. Surv.*, 55(10):203:1–203:17, 2023. doi:  
 727        10.1145/3561970. URL <https://doi.org/10.1145/3561970>.

728

729        Frederik Schmitt, Christopher Hahn, Markus N. Rabe, and Bernd Finkbeiner. Neural circuit synthesis  
 730        from specification patterns. In Marc’Aurelio Ranzato, Alina Beygelzimer, Yann N. Dauphin, Percy  
 731        Liang, and Jennifer Wortman Vaughan (eds.), *Advances in Neural Information Processing Systems*  
 732        *34: Annual Conference on Neural Information Processing Systems 2021, NeurIPS 2021, December*  
 733        *6-14, 2021, virtual*, pp. 15408–15420, 2021. URL <https://proceedings.neurips.cc/paper/2021/hash/8230bea7d54bcd99cdfe85cb07313d5-Abstract.html>.

734

735        Frederik Schmitt, Matthias Cosler, and Bernd Finkbeiner. Neural circuit synthesis with pre-trained  
 736        language models. In *First International Workshop on Deep Learning-aided Verification*, 2023.

737

738        Daniel Selsam and Nikolaj S. Bjørner. Guiding high-performance SAT solvers with unsat-core  
 739        predictions. In Mikolás Janota and Inês Lynce (eds.), *Theory and Applications of Satisfia-*  
 740        *bility Testing - SAT 2019 - 22nd International Conference, SAT 2019, Lisbon, Portugal, July*  
 741        *9-12, 2019, Proceedings*, volume 11628 of *Lecture Notes in Computer Science*, pp. 336–353.  
 742        Springer, 2019. doi: 10.1007/978-3-030-24258-9\_24. URL [https://doi.org/10.1007/978-3-030-24258-9\\_24](https://doi.org/10.1007/978-3-030-24258-9_24).

743

744        Daniel Selsam, Matthew Lamm, Benedikt Bünz, Percy Liang, Leonardo de Moura, and David L. Dill.  
 745        Learning a SAT solver from single-bit supervision. In *7th International Conference on Learning*  
 746        *Representations, ICLR 2019, New Orleans, LA, USA, May 6-9, 2019*. OpenReview.net, 2019. URL  
 747        [https://openreview.net/forum?id=HJMC\\_iA5tm](https://openreview.net/forum?id=HJMC_iA5tm).

748

749        Rico Sennrich, Barry Haddow, and Alexandra Birch. Neural machine translation of rare words  
 750        with subword units. In *Proceedings of the 54th Annual Meeting of the Association for Com-*  
 751        *putational Linguistics, ACL 2016, August 7-12, 2016, Berlin, Germany, Volume 1: Long Pa-*  
 752        *pers*. The Association for Computer Linguistics, 2016. doi: 10.18653/V1/P16-1162. URL  
 753        <https://doi.org/10.18653/v1/p16-1162>.

754        Nino Shervashidze, Pascal Schweitzer, Erik Jan van Leeuwen, Kurt Mehlhorn, and Karsten M. Borg-  
 755        wardt. Weisfeiler-lehman graph kernels. *J. Mach. Learn. Res.*, 12:2539–2561, 2011. doi: 10.5555/1953048.2078187. URL <https://dl.acm.org/doi/10.5555/1953048.2078187>.

756 Yangyang Shi, Gaël Le Lan, Varun Nagaraja, Zhaocheng Ni, Xinhao Mei, Ernie Chang, Forrest N.  
 757 Iandola, Yang Liu, and Vikas Chandra. Enhance audio generation controllability through represen-  
 758 tation similarity regularization. *CoRR*, abs/2309.08773, 2023. doi: 10.48550/ARXIV.2309.08773.  
 759 URL <https://doi.org/10.48550/arXiv.2309.08773>.

760

761 Zhengyuan Shi, Ziyang Zheng, Sadaf Khan, Jianyuan Zhong, Min Li, and Qiang Xu. Deep-  
 762 gate3: Towards scalable circuit representation learning. In Jinjun Xiong and Robert Wille  
 763 (eds.), *Proceedings of the 43rd IEEE/ACM International Conference on Computer-Aided De-  
 764 sign, ICCAD 2024, Newark Liberty International Airport Marriott, NJ, USA, October 27-  
 765 31, 2024*, pp. 184:1–184:9. ACM, 2024. doi: 10.1145/3676536.3676791. URL <https://doi.org/10.1145/3676536.3676791>.

766

767 A. Prasad Sistla and Edmund M. Clarke. The complexity of propositional linear temporal logics. *J.  
 768 ACM*, 32(3):733–749, 1985. doi: 10.1145/3828.3837. URL <https://doi.org/10.1145/3828.3837>.

769

770 Larry J. Stockmeyer. *The complexity of decision problems in automata theory and logic*. PhD thesis,  
 771 Massachusetts Institute of Technology, USA, 1974. URL <http://hdl.handle.net/1721.1/15540>.

772

773 Chi Sun, Xipeng Qiu, Yige Xu, and Xuanjing Huang. How to fine-tune BERT for text classi-  
 774 fication? In Maosong Sun, Xuanjing Huang, Heng Ji, Zhiyuan Liu, and Yang Liu (eds.),  
 775 *Chinese Computational Linguistics - 18th China National Conference, CCL 2019, Kunming,  
 776 China, October 18-20, 2019, Proceedings*, volume 11856 of *Lecture Notes in Computer Sci-  
 777 ence*, pp. 194–206. Springer, 2019. doi: 10.1007/978-3-030-32381-3\16. URL [https://doi.org/10.1007/978-3-030-32381-3\\_16](https://doi.org/10.1007/978-3-030-32381-3_16).

778

779 Aäron van den Oord, Yazhe Li, and Oriol Vinyals. Representation learning with contrastive predictive  
 780 coding. *CoRR*, abs/1807.03748, 2018. URL <http://arxiv.org/abs/1807.03748>.

781

782 Homer Walke, Daniel Ritter, Carl Trimbach, and Michael Littman. Learning finite linear temporal  
 783 logic specifications with a specialized neural operator. *CoRR*, abs/2111.04147, 2021. URL  
 784 <https://arxiv.org/abs/2111.04147>.

785

786 Thomas Wolf, Lysandre Debut, Victor Sanh, Julien Chaumond, Clement Delangue, Anthony Moi,  
 787 Pierrick Cistac, Tim Rault, Rémi Louf, Morgan Funtowicz, and Jamie Brew. Huggingface’s  
 788 transformers: State-of-the-art natural language processing. *CoRR*, abs/1910.03771, 2019. URL  
 789 <http://arxiv.org/abs/1910.03771>.

790

791 Haoyuan Wu, Haisheng Zheng, Yuan Pu, and Bei Yu. Circuit representation learning with masked  
 792 gate modeling and verilog-aig alignment. In *The Thirteenth International Conference on Learning  
 793 Representations, ICLR 2025, Singapore, April 24-28, 2025*. OpenReview.net, 2025. URL <https://openreview.net/forum?id=US9k5TXVLZ>.

794

795 Nan Wu, Yingjie Li, Hang Yang, Hanqiu Chen, Steve Dai, Cong Hao, Cunxi Yu, and Yuan Xie.  
 796 Survey of machine learning for software-assisted hardware design verification: Past, present, and  
 797 prospect. *ACM Trans. Design Autom. Electr. Syst.*, 29(4):1–42, 2024. doi: 10.1145/3661308. URL  
 798 <https://doi.org/10.1145/3661308>.

799

800 Yonghui Wu, Mike Schuster, Zhifeng Chen, Quoc V. Le, Mohammad Norouzi, Wolfgang Macherey,  
 801 Maxim Krikun, Yuan Cao, Qin Gao, Klaus Macherey, Jeff Klingner, Apurva Shah, Melvin Johnson,  
 802 Xiaobing Liu, Lukasz Kaiser, Stephan Gouws, Yoshikiyo Kato, Taku Kudo, Hideto Kazawa, Keith  
 803 Stevens, George Kurian, Nishant Patil, Wei Wang, Cliff Young, Jason Smith, Jason Riesa, Alex  
 804 Rudnick, Oriol Vinyals, Greg Corrado, Macduff Hughes, and Jeffrey Dean. Google’s neural  
 805 machine translation system: Bridging the gap between human and machine translation. *CoRR*,  
 806 abs/1609.08144, 2016. URL <http://arxiv.org/abs/1609.08144>.

807

808 Zhuofeng Wu, Sinong Wang, Jiatao Gu, Madian Khabsa, Fei Sun, and Hao Ma. CLEAR: contrastive  
 809 learning for sentence representation. *CoRR*, abs/2012.15466, 2020. URL <https://arxiv.org/abs/2012.15466>.

810 Ruiyang Xu and Karl Lieberherr. On-the-fly model checking with neural mcts. In *NASA Formal Methods: 14th International Symposium, NFM 2022, Pasadena, CA, USA, May 24–27, 2022, Proceedings*, pp. 557–575, Berlin, Heidelberg, 2022. Springer-Verlag. ISBN 978-3-031-06772-3. doi: 10.1007/978-3-031-06773-0\_30. URL [https://doi.org/10.1007/978-3-031-06773-0\\_30](https://doi.org/10.1007/978-3-031-06773-0_30).

816 Yihao Xue, Kyle Whitecross, and Baharan Mirzasoleiman. Investigating why contrastive learning  
817 benefits robustness against label noise. In Kamalika Chaudhuri, Stefanie Jegelka, Le Song, Csaba  
818 Szepesvári, Gang Niu, and Sivan Sabato (eds.), *International Conference on Machine Learning, ICML 2022, 17–23 July 2022, Baltimore, Maryland, USA*, volume 162 of *Proceedings of Machine Learning Research*, pp. 24851–24871. PMLR, 2022. URL <https://proceedings.mlr.press/v162/xue22a.html>.

822 Ziyang Zheng, Shan Huang, Jianyuan Zhong, Zhengyuan Shi, Guohao Dai, Ningyi Xu, and Qiang  
823 Xu. Deepgate4: Efficient and effective representation learning for circuit design at scale. In  
824 *The Thirteenth International Conference on Learning Representations, ICLR 2025, Singapore, April 24–28, 2025*. OpenReview.net, 2025. URL <https://openreview.net/forum?id=b101RabU9W>.

827 Keren Zhu, Hao Chen, Walker J. Turner, George F. Kokai, Po-Hsuan Wei, David Z. Pan, and Haoxing  
828 Ren. TAG: learning circuit spatial embedding from layouts. In Tulika Mitra, Evangeline F. Y.  
829 Young, and Jinjun Xiong (eds.), *Proceedings of the 41st IEEE/ACM International Conference on Computer-Aided Design, ICCAD 2022, San Diego, California, USA, 30 October 2022 – 3 November 2022*, pp. 66:1–66:9. ACM, 2022. doi: 10.1145/3508352.3549384. URL <https://doi.org/10.1145/3508352.3549384>.

834 Weijun Zhu, Huanmei Wu, and Miaolei Deng. LTL model checking based on binary classification of  
835 machine learning. *IEEE Access*, 7:135703–135719, 2019. doi: 10.1109/ACCESS.2019.2942762.  
836 URL <https://doi.org/10.1109/ACCESS.2019.2942762>.

## A LINEAR TEMPORAL LOGIC

841 Formally, LTL syntax is defined as:

$$\varphi := p \mid \varphi \wedge \varphi \mid \neg \varphi \mid \bigcirc \varphi \mid \varphi \mathcal{U} \varphi$$

845 We evaluate LTL semantics over a set of traces:  $TR := (2^{AP})^\omega$ . For a trace  $\pi \in TR$ , we denote  $\pi[0]$   
846 as the starting element of a trace  $\pi$ , and for a  $k \in \mathbb{N}$ , let  $\pi[k]$  be the  $k$ -th element of the trace  $\pi$ . With  
847  $\pi[k, \infty]$  we denote the infinite suffix of  $\pi$  starting at  $k$ . We write  $\pi \models \varphi$  for the trace  $\pi$  that satisfies  
848 the formula  $\varphi$ .

849 For a trace  $\pi \in TR$ ,  $p \in AP$ , and formulas  $\varphi$ :

- 851 •  $\pi \models \neg \varphi$  iff  $\pi \not\models \varphi$
- 852 •  $\pi \models p$  iff  $p \in \pi[0]$ ;  $\pi \models \neg p$  iff  $p \notin \pi[0]$
- 853 •  $\pi \models \varphi_1 \wedge \varphi_2$  iff  $\pi \models \varphi_1$  and  $\pi \models \varphi_2$
- 854 •  $\pi \models \bigcirc \varphi$  iff  $\pi[1, \infty] \models \varphi$
- 855 •  $\pi \models \varphi_1 \mathcal{U} \varphi_2$  iff  $\exists l \in \mathbb{N} : (\pi[l, \infty] \models \varphi_2 \wedge \forall m \in [0, l-1] : \pi[m, \infty] \models \varphi_1)$

858 We further derive several useful temporal and boolean operators. These include  $\vee$ ,  $\implies$ ,  $\Leftrightarrow$  as  
859 boolean operators and the following temporal operators:

- 861 •  $\varphi_1 \mathcal{R} \varphi_2$  (release) is defined as  $\neg(\neg \varphi_1 \mathcal{U} \neg \varphi_2)$
- 862 •  $\Box \varphi$  (globally) is defined as  $\perp \mathcal{R} \varphi$
- 863 •  $\Diamond \varphi$  (eventually) is defined as  $\top \mathcal{U} \varphi$

864 **B AIGER**  
865866 The format is based on using And-Inverter graphs to concisely describe circuits composed of AND  
867 and NOT gates, as well as simple memory cells called latches. More complex circuits are built by  
868 combining these elementary components through circuit connections. We represent these connections  
869 between inputs, outputs, gates and latches through integer-denoted variables.  
870871 

- 872 • Each circuit variable is represented by a pair of consecutive integers. Odd integers denote  
873 the negation of the variable represented by the preceding even integer. The initial variables  
874 0 and 1 represent the constant values FALSE and TRUE, respectively.
- 875 • Input and output connections are each defined by a single variable.
- 876 • AND gates are specified using three variable numbers. The first variable represents the  
877 gate’s output, which is the conjunction of the two variables represented by the remaining  
878 two numbers.
- 879 • Latches function as simple memory cells. Each latch is defined by two variable numbers:  
880 the output variable and the input variable. The output variable’s value is determined by the  
881 input variable’s value from the previous computation step. These variables are initially set  
882 to FALSE.

883 The file containing an AIGER circuit begins with a header containing the string `aag` and five numbers  
884 (`M,I,L,O,A`), each representing the size and shape of the circuit.  
885886 

- 887 • **M** : maximum variable index ( $2 \times$  number of variables)
- 888 • **I** : number of inputs
- 889 • **L** : number of latches
- 890 • **O** : number of outputs
- 891 • **A** : number of AND gates

892 Following the header, each subsequent line represents either an input, latch, output, or gate, adhering  
893 to the formatting conventions discussed in this section. After the main body containing the circuit  
894 description, there is an optional symbols table which allows for arbitrary naming of all circuit  
895 components.  
896897 **C REPRODUCIBILITY**  
898901 We rely on the PyTorch 2.3.0 (Paszke et al., 2019) and Huggingface Transformers 4.46.2 (Wolf et al.,  
902 2019) packages. We train the model on 8 NVIDIA A100-SXM4-80GB GPUs using Distributed Data  
903 Parallel and Mixed-precision (Micikevicius et al., 2017).904 We train the model for 12 epoch, with a per-GPU mini-batch size of 128 and a gradient accumulation  
905 step size of 2. We take the model at 6 epochs as the best one (roughly 110,000 steps or taking 8 hours  
906 of training time). We use AdamW (Loshchilov & Hutter, 2019) as the optimizer of choice, with the  
907 default  $\beta_1 = 0.9$ ,  $\beta_2 = 0.999$  values. The weighing parameter for the representation regularization is  
908 set to  $\lambda = 0.25$ . We initialize the learnable temperature parameter to  $\tau = 0.07$  same as in Radford  
909 et al. (2021).910 The learnable projection matrices are set to project to 1024 dimensions and are initialized in the same  
911 way as in Radford et al. (2021). We find that while going from 768 to 1024 helps the model, there are  
912 diminishing returns in increasing dimension higher than that and therefore we keep it at 1024.  
913914 We diverge from Radford et al. (2021) by keeping the logit scaling factor fixed. We use a relatively  
915 low value for the learning rate, of  $2e^{-4}$ , due to the nature of BERT models and the catastrophic  
916 forgetting problem appearing at higher values (Sun et al., 2019). We use a linear warm-up and decay  
917 scheduler policy with a warm-up period of 4200 steps and a linear decay policy to 0.

918  
919  
920  
921  
922  
923  
924  
925  
926  
927  
928  
929  
930  
931  
932  
933  
934  
935  
936  
937  
938  
939  
940  
941  
942  
943  
944  
945  
946  
947  
948  
949  
950  
951  
952  
953  
954  
955  
956  
957  
958  
959  
960  
961  
962  
963  
964  
965  
966  
967  
968  
969  
970  
971  
Table 4: Hyperparameters and Training Setup

Category	Hyperparameter	Value / Range
Hardware & Software	Framework & version	Python 3.10.12,
	CUDA	CUDA 12.3
	GPUs	8× A100-SXM4-80GB
	Random seed	580946
Training duration	Max epochs	100 ( $\approx$ 165,000 steps, $\approx$ 15 h)
	Best checkpoint	Epoch 80 ( $\approx$ 130000 steps, $\approx$ 12 h)
Batching	Per-GPU batch size	128
	Gradient accumulation	2 steps
Optimizer & LR	Optimizer	AdamW
	$\beta_1, \beta_2$	0.9, 0.999
	Weight decay	0.01
	Initial LR	$2 \times 10^{-4}$
Scheduler	Warmup steps	12000
	Decay policy	Linear to 0 over 165,000 steps
Model-specific	$\lambda$ (reg. weight)	0.25
	$\tau$ (temp. init)	0.07
	Projection dimension	1024

## D R1 - EXECUTION TIME

In Table 5 and Table 6, we provide the wall clock times for the different methods used for the cross-modal and intra-modal retrieval experiments from Section 6. Note that the wall-clock times do not differ significantly between the ML models (CodeBERT, Siamese-CNML, CNML-base), as they have the same architecture and model size for inference.

Table 5: Wall-clock time measurements over methods for intra-modal retrieval

Wall-Clock Time (s)	127 × n=100			100 × N=1000		
	Total	Mean	Std	Total	Mean	Std
Inverted Levenshtein	0.032	0.001	0.001	0.314	0.003	0.001
Bag-of-keywords	0.101	0.001	0.002	0.660	0.001	0.002
Weisfeiler–Lehman	4.232	0.033	0.002	48.520	0.485	0.055
CodeBERT	14.509	0.114	0.007	112.951	1.129	0.021
Siamese-CNML	14.459	0.114	0.007	113.130	1.131	0.027
CNML-base	14.426	0.114	0.007	112.690	1.127	0.022
<i>MC-ALL</i>	2313.234	18.214	58.100	18213.204	182.132	448.370

Table 6: Wall-clock time measurements over methods for cross-modal retrieval

Wall-Clock Time (s)	127 × n=100			100 × n=1000		
	Total	Mean	Std	Total	Mean	Std
CodeBert	14.851	0.116	0.007	115.153	1.151	0.028
Siamese-CNML	14.853	0.116	0.007	114.748	1.147	0.028
CNML-base	14.847	0.116	0.007	114.672	1.146	0.029
<i>MC-ALL</i>	2313.234	18.214	58.100	18213.204	182.132	448.370

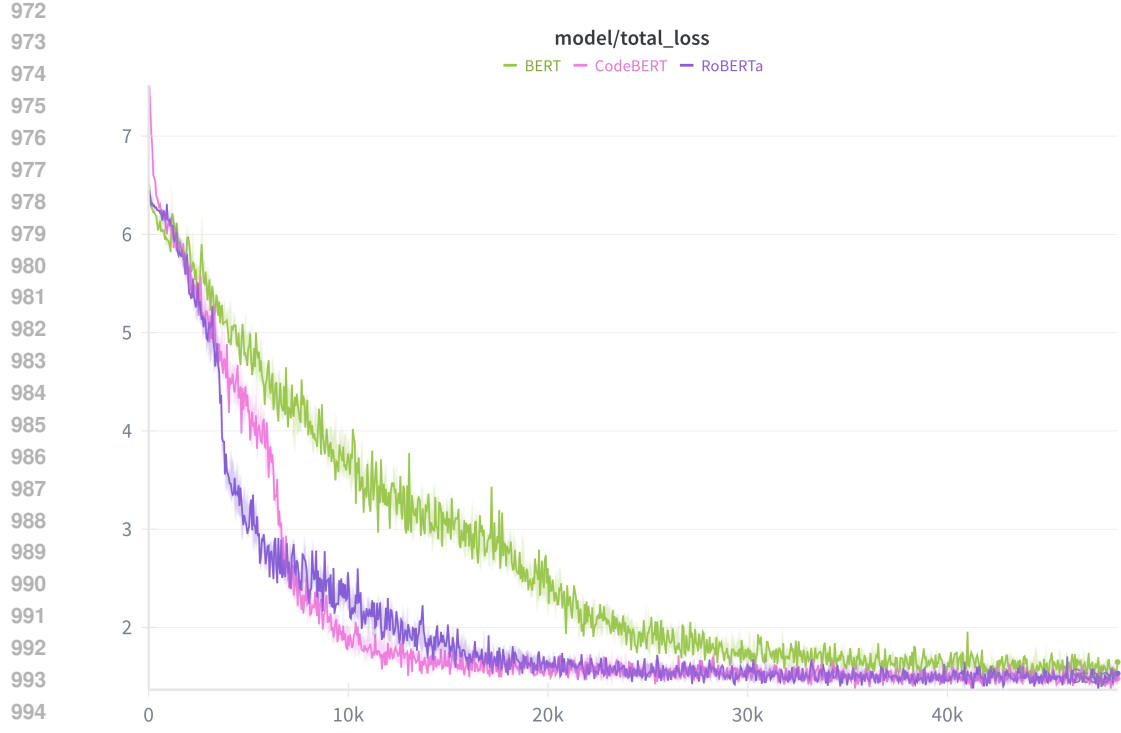


Figure 4: Loss plot of a BERT, RoBERTa, and CodeBERT models

## E R2 - COMPARISON BETWEEN BERT MODELS

In Figure 4, we compare the performance of BERT (Devlin et al., 2019), RoBERTa (Liu et al., 2019), and CodeBERT (Feng et al., 2020) models with equivalent hyperparameters over the cnml-base dataset. We find that RoBERTa achieves comparable results to CodeBert but takes longer to converge to the same loss, indicating that the code pretraining of CodeBert provides some benefits. BERT does take significantly longer to converge, and training BERT is more sensitive to hyperparameters. Additionally, the comparison with BERT is skewed as it uses WordPiece tokenization (Wu et al., 2016) while RoBERTa and CodeBert use Byte-Pair Encoding (Sennrich et al., 2016) tokenization (Devlin et al., 2019; Liu et al., 2019). Therefore, BERT’s token sequences are longer for the same input; hence, the context length of the pre-trained BERT model is de facto shorter.

## F R3 - ANALYSIS OF RANK DISTRIBUTIONS

In Figure 5 we show histograms of rank distribution and their Cumulative Frequency Distribution (CFD) for all methods for intra-modal search over the  $n = 100$  problem set.

We find that both CNML-base and CNML-simple significantly outperform the other methods, with a high concentration of ranks at low values, as demonstrated by the histogram distributions and the CFD curves. Both the neural baselines in Siamese-CNML and CodeBERT, and the algorithmic baselines in Weisfeiler-Lehman, Inverted Levenstein, and Bag-of-keyword, are behind the CNML methods’ baselines, with an almost random distribution of ranks. Although we note an interesting property of the Bag-of-keyword method, where, despite its on-average poor performance, it has no ranks in the last quintile, indicating that it does not make ‘extreme mistakes’ in ranking pairs.

## G R4 - QUALITATIVE SAMPLES

Figures 6, 7, and 8 present several qualitative samples of circuits and specifications from our dataset. The visualization of circuits, and the computation of the Manna-Pnueli hierarchy, are performed

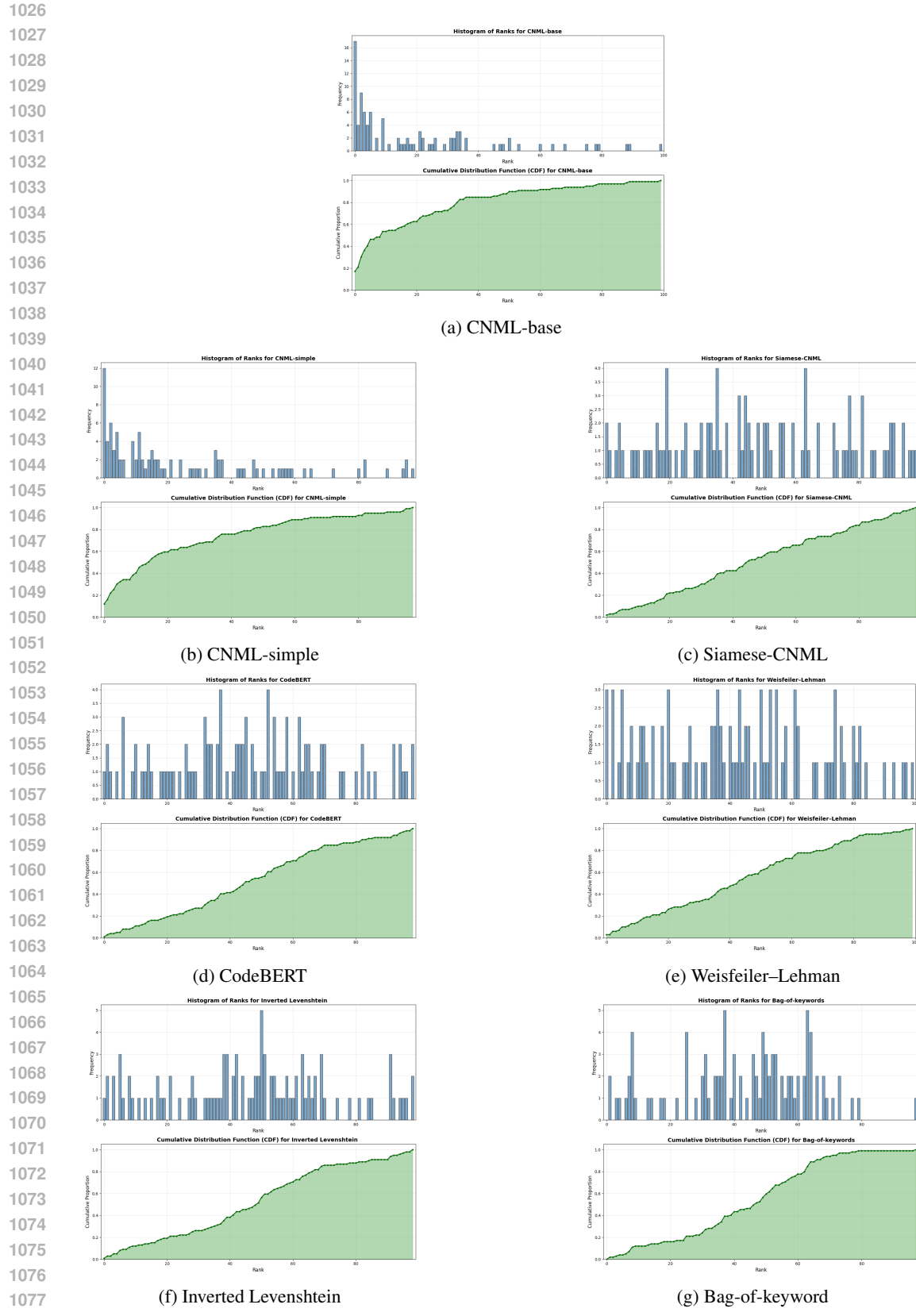


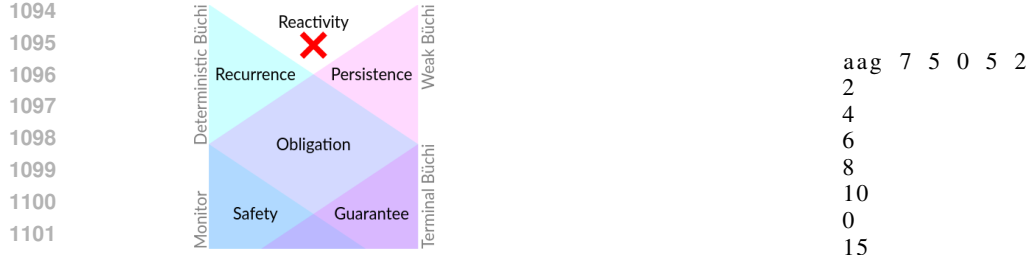
Figure 5: Rank Distribution and CFD plots for all methods

1080 using Spot (Duret-Lutz et al., 2022). Unused input and output gates are removed from the circuit  
 1081 visualization for the purposes of clarity.  
 1082

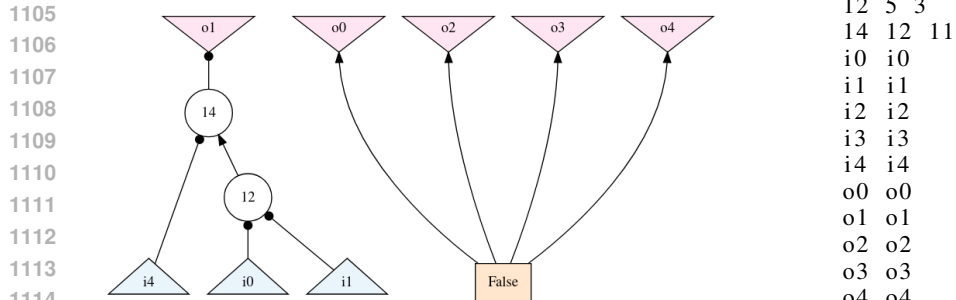
1083 The Manna-Pnueli hierarchy (Manna & Pnueli, 1990) classifies specifications in linear-time temporal  
 1084 logic into a hierarchy based on the automata complexity needed to recognize such properties. Its  
 1085 core are safety and guarantee properties. Safety properties describe behavior that can be refuted by  
 1086 a finite counterexample, such as “X never happens”. The dual of a safety property is a guarantee  
 1087 property, which describes properties such as “Y happens eventually”. The hierarchy is built through  
 1088 the Boolean combination of these classes. The most general class, reactivity, captures all  $\omega$ -regular  
 1089 properties expressible in LTL. We use this hierarchy as a means to measure the complexity of our  
 1090 specifications, with higher classes representing more intricate specifications.  
 1091

$$(((\square(\diamond(i1))) \vee (\square(\diamond(i4)))) \vee (\square(\diamond(i0)))) \leftrightarrow (\square(\diamond(o1)))$$

(a) LTL Specification



(b) Position of the specification in the Manna-Pnueli hierarchy



(c) Visual representation of the matching circuit

(d) AIGER representation

Figure 6: Example of a circuit-specification pair from cnml-base dataset

## H R5 - AMBA RESULTS

Table 7: AMBA Cross-modal Results for Different Methods and Dataset Sizes.

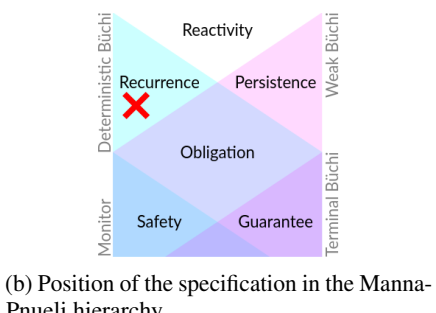
Method	12 samples of N=100			
	MRR	MR	R@1%	R@10%
CodeBERT	0.020	54.91	0.0%	0.0%
Siamese-CNML	0.018	59.91	0.0%	0.0%
CNML-simple	0.489	5.33	33.33%	75.0%
<b>CNML-base</b>	<b>0.688</b>	<b>1.41</b>	<b>58.38%</b>	<b>100%</b>

```

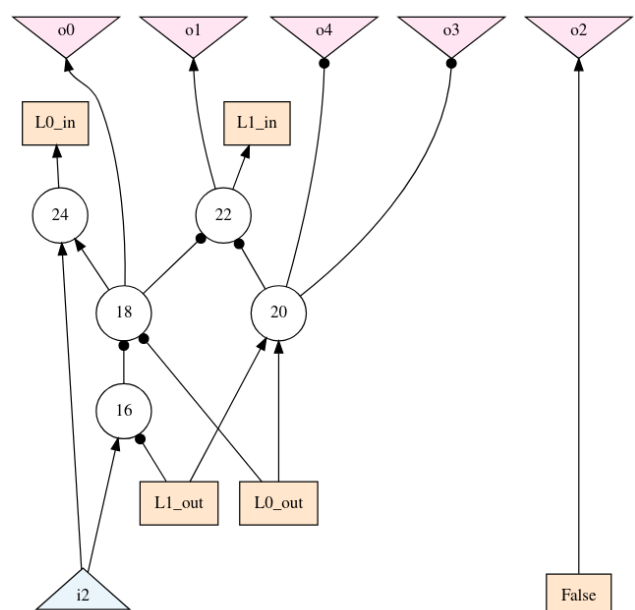
1134
1135
1136
1137
1138
1139
1140
1141      ( $\square(\Diamond((!(i1)) \vee (\bigcirc(o0)))) \wedge (\square(((o1) \wedge (!(o0))) \leftrightarrow ((!(o0)) \vee (o1)))) \wedge (\square((i2) \rightarrow (\Diamond(o1))))$ )
1142       $\wedge (\square((!(o2)) \vee (!(o4)))) \wedge (\square((((!(i3)) \wedge (i0)) \wedge (!(i2))) \wedge (i1))$ 
1143           $\rightarrow (\Diamond(((!(o1)) \wedge (o3)) \wedge (!(o2)))) \wedge (o4))))$ 
1144

```

### (a) LTL Specification



### (b) Position of the specification in the Manna-Pnueli hierarchy



(c) Visual representation of the matching circuit

```

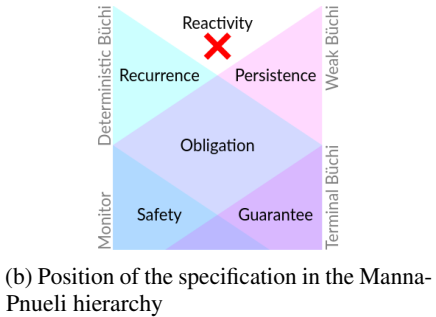
aag 12 5 2 5 5
2
4
6
8
10
12 24
14 22
18
22
0
21
21
16 6 15
18 13 17
20 12 14
22 19 21
24 6 18
i0 i0
i1 i1
i2 i2
i3 i3
i4 i4
10 10
11 11
o0 o0
o1 o1
o2 o2
o3 o3
o4 o4

```

#### (d) AIGER representation

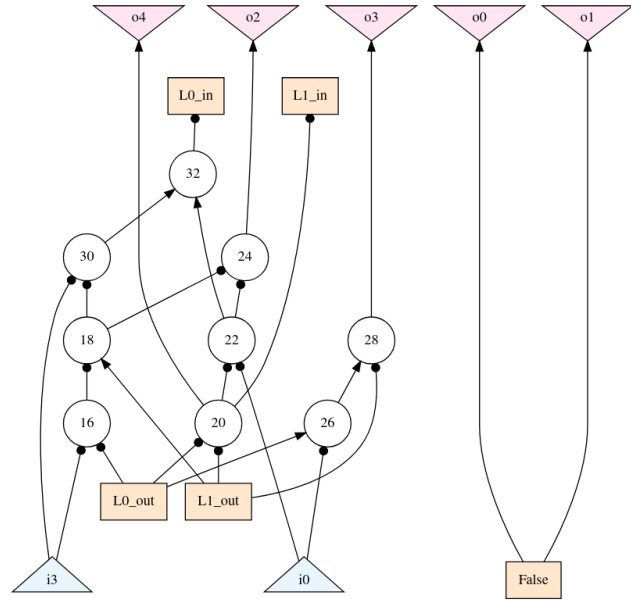
Figure 7: Example circuit-specification pair from cnml-base dataset

1188  
 1189  
 1190  
 1191  
 1192  $((i1 \wedge i2 \wedge \neg i3) \mathcal{R} (\neg o2 \vee o3 \vee \neg o4)) \wedge \square((\neg o0 \vee \neg o1) \wedge (\neg o0 \vee o3) \wedge (\neg i1 \vee \neg o0) \wedge \diamond(\neg i2 \vee o2)$   
 1193  $\wedge (\neg i4 \vee (i0 \wedge \bigcirc(\neg o0 \wedge \neg o2 \wedge o3)) \vee (\neg i0 \wedge \bigcirc(o0 \vee o2 \vee \neg o3)))$   
 1194  $\wedge (\neg o3 \vee \bigcirc(i3 \mathcal{R} ((i3 \vee o2) \wedge (i3 \vee o4))))$   
 1195  $\wedge (\neg i2 \vee \diamond o3) \wedge (i0 \vee \neg i1 \vee i2 \vee i3 \vee \diamond(\neg o1 \wedge \neg o2 \wedge o3 \wedge \neg o4)) \wedge (i4 \vee (o4 \wedge \bigcirc o4) \vee (\neg o4 \wedge \bigcirc \neg o4))$   
 1196  $\wedge (\neg o4 \vee \bigcirc(o2 \mathcal{R} o1)) \wedge (\neg i1 \vee \diamond o2)$   
 1197  $\wedge (\neg i3 \vee \bigcirc(\neg i1 \vee \bigcirc \bigcirc \bigcirc \bigcirc \bigcirc \bigcirc (o3 \wedge o4))))$   
 1198  $\vee \bigcirc \diamond((o3 \wedge ((i0 \vee i3) \mathcal{R} (\neg i0 \vee i3))) \vee (o2 \wedge ((i0 \vee i2) \mathcal{R} (i0 \vee \neg i2))))$   
 1199  
 1200  
 1201 (a) LTL formula  
 1202  
 1203  
 1204  
 1205  
 1206  
 1207  
 1208  
 1209  
 1210  
 1211 (b) Position of the specification in the Manna-Pnueli hierarchy  
 1212  
 1213  
 1214  
 1215  
 1216  
 1217  
 1218  
 1219  
 1220  
 1221  
 1222  
 1223  
 1224  
 1225  
 1226  
 1227  
 1228  
 1229  
 1230  
 1231  
 1232  
 1233  
 1234  
 1235  
 1236  
 1237  
 1238  
 1239  
 1240  
 1241



(a) LTL formula

(b) Position of the specification in the Manna-Pnueli hierarchy



(c) Visual representation of the matching circuit

aag	16	5	2	5	9
2					
4					
6					
8					
10					
12	33				
14	21				
0					
0					
24					
28					
20					
16	9	13			
18	14	17			
20	13	15			
22	3	21			
24	19	23			
26	3	12			
28	15	26			
30	9	19			
32	22	30			
i0	i0				
i1	i1				
i2	i2				
i3	i3				
i4	i4				
10	10				
11	11				
o0	o0				
o1	o1				
o2	o2				
o3	o3				
o4	o4				

(d) AIGER representation

Figure 8: Example circuit-specification pair from cnml-base dataset